Parameterizing Inanimate Agents:
The Motion of a Virtual Ball and the Behaviour of a Machine-Learning Interactive System

by

Adam Leonard Zytaruk Francey

A thesis
presented to the University Of Waterloo
in fulfilment of the
thesis requirement for the degree of
Master of Arts
in
Psychology

Waterloo, Ontario, Canada, 2021

0.1 Author's Declaration

This thesis consists of material all of which I authored or co-authored: see Statement of Contributions included in the thesis. This is a true copy of the thesis, including any required final revisions, as accepted by my examiners.

I understand that my thesis may be made electronically available to the public.

0.2 Statement of Contributions

Research presented in Chapter 3:

The machine learning algorithm and behaviour modes used in this chapter originally appear in Meng et al. (2020). Lingheng Meng, Daiwei Lin, and myself developed the algorithm under the supervision of Dr. Dana Kulić and with assistance from Dr. Rob Gorbet and Philip Beesley. I designed and implemented the behaviour modes which interact with the algorithm. Lingheng Meng and Daiwei Lin drafted the manuscript which originally contained the quote in Appendix C.2.1, with intellectual input from each author, and the quote is based on my original project design notes.

0.3 Abstract

In this thesis we parameterized interactive objects and systems and investigated their effects on perceived agency. In one experiment we developed a virtual reality simulation in which the motion path of a virtual ball is parameterized by the magnitude and direction of its jerk component. Subjects classified several motions paths into animate and inanimate categories. We found that motion paths with a large jerky deviation from our definition of an inanimate zero jerk motion path, per the subject's physical point of view, are classified as animate by the subject. In another experiment, we developed a Living Architecture System whose interactive behaviours are defined by a set of modifiable control parameters. We focused on two behaviour modes which are differentiated by the usage of these control parameters: one in which static values were hand-picked to produce what we had determined to be aesthetically interesting interactive behaviour, and one in which a machine learning algorithm assumes full real-time control of each parameter with restrictions. We measured the subject's experience with skin-conductance and brain activity before and after exposure to one of the behaviour modes and follow with a questionnaire. We found that, after exposure, subjects who experienced static parameters had a decrease in skin-conductance while subjects who experienced the machine learning algorithm had an increase in skin-conductance. However, the statistically significant results of the second experiment remain inconclusive because of the small sample set.

0.4 Acknowledgements

Thanks to Colin Ellard for bravely supervising a research student with training in mathematics rather than psychology, and for the rest of Urban Realities Laboratory for extremely helpful input on my direction, the statistics used, and for being my software testing guinea pigs:

> Dr. Hanna Negami, Emily Grant, Dr. Robin Mazumder, Jatheesh Srikantharajah, David Borkenhagen, Dr. Vedran Dzebic, Richard Marion

Thanks to Alex Esser for helping with data collection for Experiment 1 and Lingheng Meng and Daiwei Lin with data collection for Experiment 2.

Thanks to Philip Beesley for immersing me so heavily is his architecture studio so that I could have full control over my research project involving Living Architecture Systems, the studio team for working so hard to ensure I had a testbed to develop:

> Mehreen Ali, Lorena Almaraz, Chelsea Attong, Anca Badut, Gabriella Bevilacqua, Timothy Boll, Alice Choupeaux, Timara Douglas, Farzaneh Victoria Fard, Mark Francis, Carolina Garcia, Maxime Gordon, Karen Zwart Hielema, Hanyang Hu, Mike Zheh Hu, Maite Iribarren, Joey Jacobson, Nicole Jazwiec, David Kadish, Pedram Karimi, Saffiya Kherraj, Luke Kimmerer, Mandeep Mangat, Nikola Miloradovic, Salvador Miranda, Richard Mui, Reza Nik, Evan Pavka, Anne Paxton, Tak Pham, Jordan Prosser, Lily Ray, Iris Redinger, Severyn Romanskyy, Nathanael Scheffler, Adam Schwartzentruber, Aleksandra Simic, Matthew Spremulli, Tania Thompson, Penny Unni, Lise van Overbeeke, Darcie Watson, Alex Willms, Guyi Yi

those on the engineering team who found themselves under my direct guidance for their extraordinary help and commitment toward my goals:

> Felicity Chan, Siddhant Chandgadkar, Charlotte Dyck, Pari Kumar, Kevin Lam, Daiwei Lin, Amber Ma, Wenlong Meng, Amir Rostami, Filip Vranes

and Living Architecture Systems Group collaborators for turning a lot of art into a lot of science:

> Andreas Beuckle, Dr. Katy Börner, Salvador Breed, Dr. Rob Gorbet, Matt Gorbet, Poul Holleman, Dr. Dana Kulić, Daiwei Lin, Lingheng Meng, Alex Young

Thanks to Mom, Dad, Eric, my family, and my friends for years of unwavering support.

Contents

0.1 Author's Declaration . . . ii
0.2 Statement of Contributions . . . iii
0.3 Abstract . . . iv
0.4 Acknowledgements . . . v
0.5 List of Figures . . . viii
0.6 List of Tables . . . ix

1 Introduction **1**
1.1 Agents . . . 1
1.2 Mechanisms . . . 1
1.3 Research Questions . . . 2

2 Effect of Trajectory with a Single Virtual Ball **3**
2.1 Subjects . . . 4
2.2 Equipment . . . 4
2.3 Stimuli: Thirty Motion Paths . . . 5
2.4 Procedure . . . 5
2.5 Analysis . . . 5
2.5.1 Zero Jerk . . . 6
2.5.2 Sinusoidal Jerk . . . 6
2.5.3 Constant Jerk . . . 7
2.6 Discussion . . . 9
2.6.1 Inanimate Trajectories . . . 9
2.6.2 Animate Trajectories . . . 9
2.6.3 Conclusion . . . 10

3 Effect of Machine Learning with an Interactive System **11**
3.1 Subjects . . . 12
3.2 Equipment . . . 12
3.3 Stimuli: Two Behaviour Modes of Aegis . . . 13
3.4 Procedure . . . 13
3.5 Analysis: SCL . . . 14
3.5.1 Data Preparation and Parameters . . . 14
3.5.2 Results: Mean . . . 14
3.5.3 Results: Slope . . . 16
3.6 Analysis: EEG . . . 16
3.6.1 Data Preparation and Parameters . . . 16
3.6.2 Summary of Results . . . 17
3.7 Analysis: Subjective Experience Questionnaire . . . 18
3.8 Discussion . . . 18
3.8.1 Results . . . 18
3.8.2 Efficacy of Mobile Biometrics . . . 18

4 General Discussion **20**

Bibliography **21**

A Statistical Analysis Methods **25**
A.1 Required R Packages 25
A.2 Step-by-step 25
A.3 Explicit Description of Models Used in this Thesis 26
A.4 Notes on Experiment 1 Analysis 27
A.5 Notes on Experiment 2 Analysis 28

B Effective Nyquist Frequency of Evenly Sampled Time-Series with Gaps **29**

C Materials **30**
C.1 Experiment 1: Simulation Space and Stimuli Details 30
C.1.1 Notation 30
C.1.2 Positioning 30
C.1.3 Initial Conditions 31
C.1.4 Base Equations of Motion 31
C.1.5 Motion Paths with Zero Jerk 31
C.1.6 Motion Paths with Sinusoidal Jerk 32
C.1.7 Motion Paths with Constant Jerk 32
C.2 Experiment 2 33
C.2.1 Interactive Behaviour and Parameters of Aegis 33
C.2.2 Subjective Experience Questionnaire 34

0.5 List of Figures

2.1 A view from inside the simulation after the retracting panel has slid upwards. The black ball is currently travelling along a predetermined motion path toward the viewer. The ball starts its path behind and below the wall, preventing the subject from guessing that its motion has any direct source. 4
2.2 Subject classification of motion paths for each type of sinusoidal jerk. Each effect is compared to the column labelled MEAN. $*** = p < .001$. 7
2.3 Subject classification of motion paths for each type of constant jerk. Each effect is compared to the column labelled MEAN. $** = p < .01$. 9

3.1 A studio member poses with Aegis. Transforming Space - Royal Ontario Museum, Toronto, Canada, 2018. Photo © Philip Beesley Studio Inc. 12
3.2 Interaction effect between behaviour group (between subjects; PB with fixed parameters and PLA with parameters varying within the ranges in Table C.2 according to the machine learning agent) and recording time (within subjects; before and after exposure) on mean SCL. Each line on the plot corresponds to a single subject and connects their *pre* and *post* values (note that one subject only has usable data in the *post* time). 16

0.6 List of Tables

2.1 Sinusoidal Jerk: Model Comparison Characteristics 6
2.2 Sinusoidal Jerk: Likelihood Ratio Tests 6
2.3 Sinusoidal Jerk: Fixed Effects 7
2.4 Constant Jerk: Model Comparison Characteristics 7
2.5 Constant Jerk: Likelihood Ratio Tests 8
2.6 Constant Jerk: Fixed Effects 8

3.1 Mean SCL: Model Comparison Characteristics 14
3.2 Mean SCL: Fixed Effects 15

A.1 General Models 27
A.2 Experiment 2: Models 28

C.1 Directions of Constant Jerk Stimuli 32
C.2 Prescripted Behaviour Parameters 33

Chapter 1

Introduction

1.1 Agents

It is reasonable to assume that humans can make sense of their world by believing that entities in their environment are guided by rational intentions (Dennett, 1971). Seminal research demonstrates that simple moving geometric shapes are described as having various intentions (Heider and Simmel, 1944), and that human actions are perceived even when most of the visual input is reduced to abstract moving point-light displays (Johansson, 1973). These ideas have spawned a field of research broadly investigating human understanding of agents in their environment. The quality of agency is typically used to describe whatever it is that separates objects like us from objects that do not have the mechanical, actional, and cognitive properties that we do (Leslie, 1995).

The related concept of animacy refers to the narrower class of biological agents. Aside from obvious visual clues, like having a face, an object may be perceived as an animate agent when it moves as if it was self-propelled (Giorgio et al., 2017), its movement indicates goal-oriented behaviour such as chasing (Gao et al., 2009) or predatory stalking (Gao et al., 2010), or it is able to be interacted with (Fukuda and Ueda, 2010). This does not solely depend on visual cues as even a moving sound has been shown to invoke the perception of animacy (Nielsen et al., 2015).

Agency has been a challenge to concretely define yet unmistakeable in nature: sticks and stones are not in the same group as snakes and dogs. With sufficient trickery virtually any object, animate or inanimate, can appear to have agency. The work presented in this thesis parameterizes my own attempt at such trickery with a ball and a robot while examining the effects on human behaviour.

1.2 Mechanisms

When studying agency detection we seek to understand the interrelation between the brain's ability to parse sensory input, interpret observed actions, and infer the social content of our environment. A well-supported theory of action perception and understanding in primates invokes the mirror neuron system (MNS); certain neurons in areas of the brain responsible for the performance of an action, such as the premotor cortex, also activate when viewing another perform that action (Gallese et al., 1996; Rizzolatti et al., 1996; di Pellegrino et al., 1992) (Bonini, 2017, for review). These actions need not be from a biological organism and the MNS activates even when observing robots (Gazzola et al., 2007). It is suspected that a similar mechanism forms the neurological basis of agency detection as brain areas responsible for intentions and emotions are activated when observing them in others (Iacoboni et al., 2005; Gallese et al., 2004).

While this evidence points toward an ability to simulate the actions and intentions of others in order to understand them, other findings suggest that inferential processes outside of the MNS are required (Saxe, 2005), especially when comparing animates to inanimates (Wheatley et al., 2007) and when the observed actions are unfamiliar or unusual (Brass et al., 2007).

1.3 Research Questions

In this thesis we parameterize interactive objects and systems and investigate their effects on perceived agency. In one experiment we developed a virtual reality simulation in which the motion path of a virtual ball is parameterized by the magnitude and direction of its jerk component. Subjects classified several motion paths into animate and inanimate categories. In another experiment, we developed a Living Architecture System whose interactive behaviours are defined by a set of modifiable control parameters. We focus on two behaviour modes which are differentiated by the usage of these control parameters: one in which static values were hand-picked to produce what we had determined to be aesthetically interesting interactive behaviour, and one in which a machine learning algorithm assumes full real-time control of each parameter with restrictions.

Software developed for this thesis was written in Python, C++, C#, Java, and R. This document was created with LaTeX.

Chapter 2

Effect of Trajectory with a Single Virtual Ball

Natural laws of our environment mandate a natural reference state of motion: things fall down and not up. Our brain structure is tuned for gravity (Vaziri and Connor, 2016) and we are sensitive to gravity even as an infant (Kim and Spelke, 2008). Our perception of motion and animacy has a special relationship to the vertical components of motion when it violates a notion of natural or Newtonian movements that rely on gravity (Scaleia et al., 2014; Chang and Troje, 2009; Tremoulet and Feldman, 2000; Gelman et al., 1995) and we are sensitive to large enough violations (Kaiser and Proffitt, 1987). Research with simple geometric shapes makes it clear that our perception of agency based on motion does not require any explicitly anthropomorphic or animate qualities (Szego and Rutherford, 2007, 2008; Tremoulet and Feldman, 2000, 2006; Opfer, 2002; Scholl and Tremoulet, 2000; Santos et al., 2008).

For this experiment we developed a rigorous definition of inanimate motion from which we built upon to contrast with suspected animate motion types. I modelled an inanimate object as one which cannot resist the natural forces in its environment and only moves according to our so-called natural reference state of motion. In the controlled laboratory environment, where gravity is the only force acting upon an object, inanimate movement equates to simple quadratic curves through space (see Appendix C.1.4, Base Equations of Motion). Importantly, this type of motion has a constant acceleration: a constant downward acceleration from gravity and zero acceleration in all other directions. In technical jargon we can say that the third time-derivative of displacement[1], called jerk, is equal to zero. Given this description of inanimate motion one might rightfully wonder about objects whose motion has a non-zero jerk. After all, objects which deviate from the inanimate trajectory cannot reach a different jerkless trajectory instantaneously so they must undergo jerky motion for some amount of time. Are these the objects that are perceived as animate?

The experiment immersed the subject in virtual reality, allowing us to display any trajectory we can calculate. The subject classified thirty motion paths by viewing a single ball traverse each motion path, in random order, and answering the question "Is this an inanimate object or a thinking being?" for each. The subject was told that each ball represents the centre of mass of some object that is either an inanimate object or a thinking being; this is a deception as all trajectories were calculated by the researcher and not the recorded movements of any inanimate object or thinking being. To prevent any direct effect of some perceived cause of the motion, in which case self-propulsion might be automatically ruled out without regard for the motion path being tested, the beginning of the object's motion path was occluded so the subject cannot see what starts the ball's motion.

[1] A.K.A. the first time-derivative of acceleration. Aside from the familiar ones, most of these quantities are rarely used but here is a list of all n-th derivatives of displacement with names that I am aware of (from $n = -7$ to $n = 6$): absop, absackle, absnap, abserk, abseleration (Mann and Janzen, 2014), absity, absement (Mann et al., 2006), displacement, velocity, acceleration, jerk, snap (jounce), crackle (flounce), pop (pounce).

The following effects on perceived animacy are investigated:

1. The effect of a higher or lower gravitational constant.

2. The effect of magnitude and dimension of sinusoidal jerk: the object's acceleration is sinusoidally time-dependent[2]. This type of motion may be roughly approximated by the periodic (oscillating) motion of a bird flying, a monkey swinging, or a human walking.

3. The effect of magnitude and direction of constant jerk: the object's acceleration is linearly time-dependent. This type of motion may be accomplished by attaching an increasingly powerful rocket to one side of an object, or by pressing down your car's accelerometer at a constant rate.

Figure 2.1: A view from inside the simulation after the retracting panel has slid upwards. The black ball is currently travelling along a predetermined motion path toward the viewer. The ball starts its path behind and below the wall, preventing the subject from guessing that its motion has any direct source.

2.1 Subjects

Forty University of Waterloo undergraduate students were recruited from SONA, and thirty subjects were included in the analysis after ten subjects were removed: five subjects experienced technical difficulties, two subjects were unfamiliar with the word "inanimate", and three subjects answered "inanimate object" for every single trial.

2.2 Equipment

Subjects wore an HTC Vive Head Mounted Display (HMD). Simulations were built and run with Unity.

[2]The jerk is also sinusoidally time-dependent. In fact, this type of motion has an infinite cascade of non-zero time-derivatives!

2.3 Stimuli: Thirty Motion Paths

Appendix C.1 defines the simulation space in detail and contains the explicit description of the motion paths presented as stimuli in the experiment. Here we give a brief description of the stimuli used to test each effect described in the introduction of this chapter. Motion paths are broken into three groups. Each group contains every combination of paths for the given regressors:

- Three paths of zero jerk (modified gravity): low gravity, normal gravity, high gravity
- Nine paths of sinusoidal jerk: magnitude (low, medium, high) $\times$ dimension (left/right, up/down, away/toward)
- Eighteen paths of constant jerk: magnitude (low, medium, high) $\times$ direction (left, right, up, down, away, toward)

2.4 Procedure

The subject is equipped with the HMD and is immersed in the virtual environment: a small rectangular room modelled after PAS 2276 at the University of Waterloo, the physical space where the experiment takes place[3]. A visible retracting panel is in the top-middle of one wall. The subject navigates to each corner of the room to get used to moving in VR and then stands on an X marked on the ground near the wall opposite the retracting panel. The instructions given in the initial briefing are reiterated. The subject will stand on the X and face the retracting panel. When the subject is steady, the experimenter presses a button to start the following process:

1. after five seconds, the slot opens
2. after one second, the ball comes out of the slot on a predetermined trajectory
3. the subject attempts to get in the way of the object's path
4. the ball reaches the end of its trajectory and the slot closes
5. the subject is asked and responds verbally, "Is this an inanimate object or a thinking being?"
6. the subject moves back to the X and is asked to focus their attention to the slot

This process is followed for all thirty randomly ordered experimental trials each presenting a single black ball with a distinct motion path. Each subject views all thirty motion paths. The experiment terminates once all motion paths have been presented.

2.5 Analysis

The analysis utilizes a series of logistic generalized linear mixed models (GLMMs) according to the process outlined in Appendix A.2. In all analyses the dependent variable (`response`) is the binary answer to the question "Is this an inanimate object or thinking being?", with "inanimate object" = 0 and "thinking being" = 1. Regressors are the categorical variables `magnitude` and `dimension/direction` described in Section 2.3.

[3]If COVID-19 weren't blocking my access I would have given the exact dimensions of the simulated room here.

2.5.1 Zero Jerk

The analysis compares low gravity and high gravity to regular gravity (intercept).

In these models, adding the magnitude variable did not significantly improve the model fit, and resulted in a larger Akaike information criterion (AIC). No significant coefficients were observed with normal gravity as the reference level in a dummy coded regression.

2.5.2 Sinusoidal Jerk

Random Effects and Model Selection

The intraclass correlation (ICC) indicates that 9.18% of model variance is explained by subject grouping. Likelihood ratio tests show that a model including both magnitude and dimension has the lowest AIC and is a significantly better fit compared to a model containing only magnitude or only dimension. Model comparisons and tests are shown in Table 2.1 and Table 2.2. Therefore the analysis will consider the GLMM which subscribes to the formula

$$\texttt{response} \sim \texttt{magnitude + dimension + 1|subject}$$

Table 2.1: Sinusoidal Jerk: Model Comparison Characteristics

Model	Formula	AIC	logLik	deviance
i (null)	$Y \sim 1 + (1\|S)$	361.41	-178.71	357.41
ii (dimension only)	$Y \sim D + (1\|S)$	293.17	-142.58	285.17
iii (magnitude only)	$Y \sim M + (1\|S)$	348.49	-170.25	340.49
iv (magnitude and dimension)	$Y \sim M + D + (1\|S)$	272.53	-130.27	260.53

Table 2.2: Sinusoidal Jerk: Likelihood Ratio Tests

Effect	Models	χ^2	p	Significance
Magnitude	ii vs. iv	24.636	$< .001$	***
Direction	iii vs. iv	79.962	$< .001$	***

$* = p < .05$, $** = p < .01$, $*** = p < .001$

Summary of Effects

Wald tests of the fixed model coefficients (Table 2.3 and Figure 2.2) to compare the response at each level of magnitude and each dimension to the average response (grand mean) indicated significant main effects of magnitude and dimension:

- motion paths with **low magnitude** sinusoidal jerk are significantly **less** likely to be classified as thinking beings
- motion paths with **high magnitude** sinusoidal jerk are significantly **more** likely to be classified as thinking beings
- motion paths with **left/right** sinusoidal jerk are significantly **more** likely to be classified as thinking beings
- motion paths with **away/toward** sinusoidal jerk are significantly **less** likely to be classified as thinking beings

Table 2.3: Sinusoidal Jerk: Fixed Effects

Effect	Estimate	SE	z	p	Sig
(Intercept)	-0.05501	0.27406	-0.201	.84	
low	-0.8384	0.2437	-3.441	$< .001$	***
medium	-0.28343	0.23063	-1.229	.22	
high	1.12184	0.25274	4.439	$< .001$	***
left/right	1.8902	0.2829	6.682	$< .001$	***
up/down	-0.10751	0.22186	-0.485	.63	
away/toward	-1.78265	0.27757	-6.422	$< .001$	***

$* = p < .05$, $** = p < .01$, $*** = p < .001$

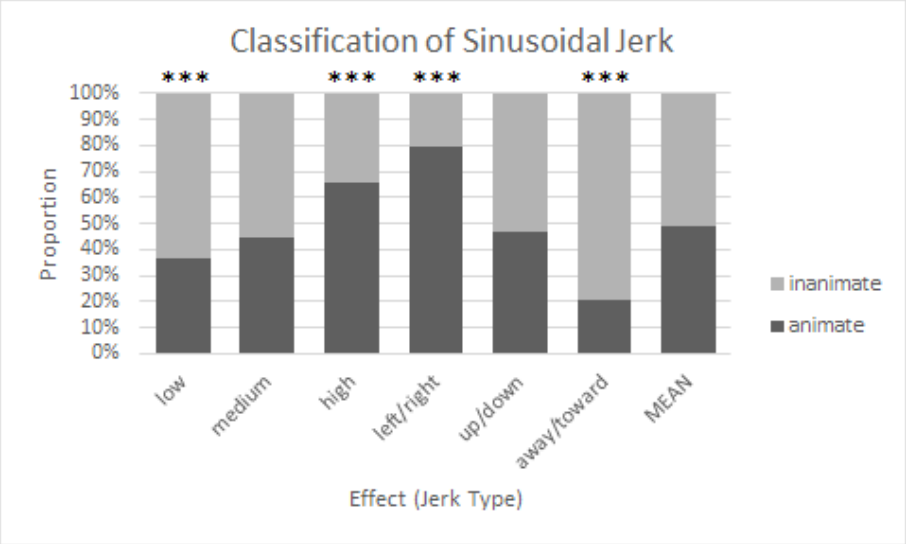

Figure 2.2: Subject classification of motion paths for each type of sinusoidal jerk. Each effect is compared to the column labelled MEAN. $*** = p < .001$.

2.5.3 Constant Jerk

Random Effects and Model Selection

The ICC indicates that 34.10% of model variance is explained by subject grouping. Likelihood ratio tests show that a model including both magnitude and direction has the lowest AIC and is a significantly better fit compared to a model containing only magnitude or only direction. Model comparisons and tests are shown in Table 2.4 and Table 2.5. Therefore the analysis will consider the GLMM which subscribes to the formula

$$\texttt{response} \sim \texttt{magnitude + direction + 1|subject}$$

Table 2.4: Constant Jerk: Model Comparison Characteristics

Model	Formula	AIC	logLik	deviance
i (null)	$Y \sim 1 + (1\|S)$	367.38	-181.69	363.38
ii (direction only)	$Y \sim D + (1\|S)$	359.41	-172.71	345.41
iii (magnitude only)	$Y \sim M + (1\|S)$	363.92	-177.96	355.92
iv (magnitude and direction)	$Y \sim M + D + (1\|S)$	355.48	-168.74	337.48

Table 2.5: Constant Jerk: Likelihood Ratio Tests

Effect	Models	χ^2	p	Significance
Magnitude	ii vs. iv	7.9361	.02	*
Direction	iii vs. iv	18.448	.002	**

$* = p < .05$, $** = p < .01$, $*** = p < .001$

Summary of Effects

Wald tests of the fixed model coefficients (Table 2.6 and Figure 2.3) to compare the response at each level of magnitude and each direction to the average response (grand mean) indicated significant main effects of magnitude and direction:

- motion paths with **high magnitude** constant jerk are significantly **more** likely to be classified as thinking beings

- motion paths with **left** or **right** constant jerk are significantly **more** likely to be classified as thinking beings

Table 2.6: Constant Jerk: Fixed Effects

Effect	Estimate	SE	z	p	Sig
(Intercept)	-2.7356	0.3775	-7.246	$< .001$	***
low	-0.3965	0.2260	-1.754	.08	
medium	-0.1640	0.2176	-0.754	.45	
high	0.5605	0.2028	2.764	.006	**
left	0.8452	0.2955	2.860	.004	**
up	-0.6905	0.4022	-1.717	.09	
away	-0.3280	0.3643	-0.900	.37	
right	0.8452	0.2955	2.860	.004	**
down	-0.1733	0.3508	-0.494	.62	
toward	-0.4986	0.3810	-1.309	.19	

$* = p < .05$, $** = p < .01$, $*** = p < .001$

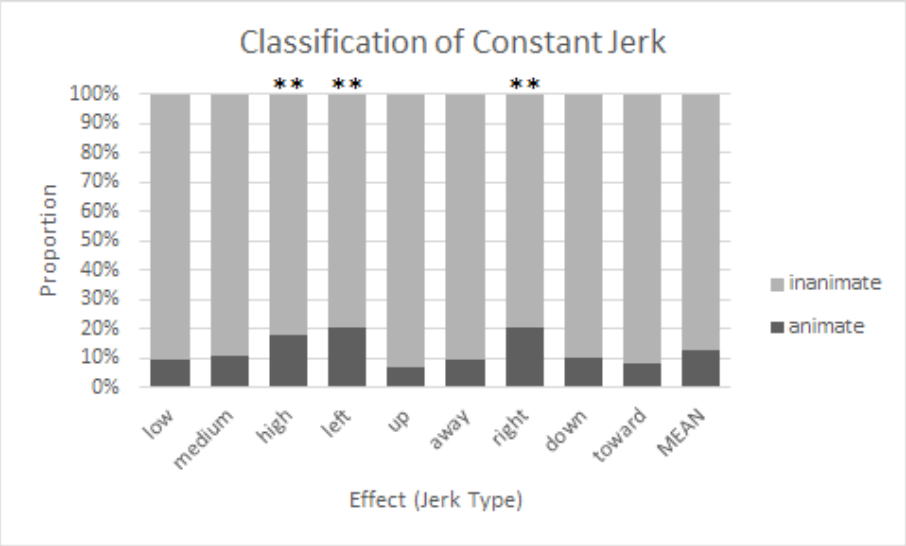

Figure 2.3: Subject classification of motion paths for each type of constant jerk. Each effect is compared to the column labelled MEAN. $** = p < .01$.

2.6 Discussion

2.6.1 Inanimate Trajectories

Some trajectories with sinusoidal jerk are described as inanimate: those with a low amount of jerk and those which jerk away or toward the subject. In both cases the motion is difficult to visually distinguish from inanimate motion; the low jerk condition only slightly deviates from a parabolic arc, and jerking away/toward results in a deviation normal[4] to the subject's plane of view which obscures the movement. Although we did not perform any statistical tests of the difference between sinusoidal and constant jerk motion paths, notice that a great majority of subjects rated constant jerk paths as inanimate while the grand mean response for sinusoidal paths is nearly evenly split.

2.6.2 Animate Trajectories

It has been shown that humans treat balls in much the same way that they treat human characters and that they are more sensitive to horizontal[5] deviations when watching human characters undergo "ballistic trajectories"[6] (Reitsma et al., 2008; Reitsma and Pollard, 2003). Correspondingly, we found that trajectories with large magnitude jerk and trajectories which jerk to the left and right are described as animate. These trajectories correspond to a large deviation from a purely inanimate trajectory. The trajectories with left and right jerk have the greatest visual deviation from the perspective of the subject.

[4]For those that may be unfamiliar with the mathematical definition of normal, a line that is normal to a 2-dimensional plane points perpendicularly away from the plane.

[5]On a 2-dimensional screen, so this means the left/right horizontal rather than the additional away/toward horizontal available in three dimensions.

[6]Another word for parabolic trajectories.

2.6.3 Conclusion

When making these classifications, the binary choice forced the subject to choose animate or inanimate even if neither choice fits perfectly. Perhaps the motion paths that are similar to our inanimate motion path are perceived to be an inanimate object, and the paths with more jerk are chosen as thinking beings only because the subject has no other option. Since any object is necessarily one or the other it does not seem rational to expand the question to include a range from inanimate to animate, however, simply adding an "I don't know" option may have given a clearer picture. It would be a good idea to probe the subject on their perception of each motion path's level of self-propulsion or goal-oriented behaviour. A future version of this study might also include chaotic paths, which are not generally travelled by inanimate objects without external forces nor deliberately travelled by thinking beings.

A growing number of motion descriptors have been shown to increase the perception of agency and animacy of a single object, including faster speeds (Szego and Rutherford, 2007), changes in direction, and acceleration (Tremoulet and Feldman, 2000). In this work we parameterized changes to acceleration and add jerk to this list. We used virtual reality to allow a subject to experience a motion path in three dimensions rather than a 2-dimensional screen. Apparent violations of gravity have been shown to increase perceptions of animacy on a 2-dimensional screen (Szego and Rutherford, 2008) and our use of virtual reality allowed us to draw upon a much more innate, salient, and physical gravitational context to test animate motion paths. The results of this experiment show that an object displaying a large deviation from inanimate motion, with the deviation being a non-zero jerk in this gravitational context, results in a simple geometric object seemingly coming to life and being classified as animate.

Chapter 3

Effect of Machine Learning with an Interactive System

Children and adults perceive animacy in robots and are willing to interact with them as if they were agents (Beran et al., 2011; Weiss et al., 2010). Living Architecture Systems (LAS), a research group based at the University of Waterloo which builds real-time interactive electronic sculptures, provides the groundwork for the current experiment by having people interact with a "curiosity-based [machine] learning algorithm (CBLA)" operating on a network of sensors and actuators (Chan et al., 2015; Gorbet et al., 2015). The current experiment is a result of my collaboration[1] with researchers in the School of Architecture[2], Department of Electrical and Computer Engineering[3], Department of Knowledge Integration[4], and 4DSOUND[5] to develop the subsequent generation of living architecture described in Meng et al. (2020). Although the philosophy is similar, this system is almost entirely different from the previous generation in hardware and software and does not use CBLA.

The experiment had museum visitors interact with *Aegis*, a living architecture system on exhibition at the Royal Ontario Museum. You can find pictures and videos of Aegis when searching the internet for the exhibit name: *Philip Beesley: Transforming Space*[6][7][8][9]. Aegis operates on input from an array of infrared (IR) proximity sensors and produces emergent interactive behaviour in its light-emitting diodes (LEDs), speakers, vibrating fronds (which we call "moths"), and curling shape memory alloy (SMA) appendages. Modifiable parameters control the timing and intensities of the behaviour patterns. In normal operation we choose static parameter values which result in aesthetically interesting behaviours. For the experiment, we took our hands off and allowed the machine learning algorithm developed in Meng et al. (2020) to modify parameters on-the-fly. Experiments were done at the end of Aegis's life, after it had spent several weeks learning. We measured the electrodermal activity (skin-conductance level; SCL) and brainwaves (electroencephalogram; EEG) of each subject, followed by a questionnaire to determine their subjective perception of agency. Processing of physiological signals is performed with

[1] In this collaboration I acted as the primary software developer.
[2] livingarchitecturesystems.com
[3] uwaterloo.ca/adaptive-systems
[4] uwaterloo.ca/knowledge-integration/
[5] 4dsound.net
[6] http://philipbeesleyarchitect.com/sculptures/ROM/index.php
[7] https://www.rom.on.ca/en/exhibitions-galleries/exhibitions/philip-beesley-transforming-space
[8] https://www.youtube.com/watch?v=SR5RJzMCvY8
[9] The living architecture system constutites a sort of distributed "consciousness". It has one central brain and additional computational power provided by microcontrollers in local clusters. It doesn't think like a human; more like an octopus.

EDA Inspector[10] (Francey, 2020a) and its companion program *EEGProcessor.py*[11][12] (Francey, 2020b).

Figure 3.1: A studio member poses with Aegis. Transforming Space - Royal Ontario Museum, Toronto, Canada, 2018. Photo © Philip Beesley Studio Inc.

3.1 Subjects

The experiment was advertised on Twitter and members of the Philip Beesley Architect Inc. volunteer pool were invited by email. Visitors to the museum could also participate by speaking to the researcher. Twenty-three subjects participated in the experiment. Twenty-two subjects completed the subjective experience questionnaire (16 female, mean age: 33.19, sd age: 11.012, one subject did not disclose age). Fourteen subjects took part while wearing physiological sensing equipment (10 female, mean age: 34, sd: 10.263).

3.2 Equipment

EEG was recorded with an InteraXon Muse Brain-Sensing Headband which measures at four locations corresponding to the 10-20 system locations Af7, Af8, Tp9 and Tp10 with a reference

[10] Processing 3.5.4.

[11] Python 3

[12] Despite the names, *EDA Inspector* can also inspect EEG signals, and *EEGProcessor.py* can also process EDA signals.

electrode at Fpz. Skin-conductance was recorded with an Empatica E4 which measures from the wrist.

3.3 Stimuli: Two Behaviour Modes of Aegis

Aegis's base behaviour is defined in Meng et al. (2020) (pp. 8-9). When nobody is interacting with Aegis, its various actuators will randomly fire either as a single action, such as an LED activating, or as a predefined pattern such as multiple LEDs activating in sequence. When somebody interacts with Aegis by coming within a few inches of a proximity detector, a pattern of activation involving all of the actuators radiates away from the triggered proximity detector. A full description of the interactive behaviour and modifiable parameters is given in Appendix C.2.1.

Two of Aegis's behaviour modes were chosen as stimuli for the experiment: Prescripted Behaviour (PB) and Parameterized Learning Agent (PLA). PB consists of a set of fixed parameter values for Aegis that create an interesting experience for the visitor by simulating an intelligent system. PLA[13] exposes the control parameters to the algorithm developed in Meng et al. (2020). The goal of this algorithm is to maximize "user engagement" by operating on the distance recorded by the proximity sensors. Roughly, user engagement increases if more visitors spend more time closer to the system. To accomplish this, PLA varies the control parameters every two seconds while searching for the optimal set.

PB and PLA have similar functions with the main distinction being fixed parameters or parameters that vary with the state of the machine learning agent, respectively. The overall pattern of activation was the same but differed in timing and intensity. For example, when a proximity sensor is triggered an LED will always fade up to some brightness over some duration, hold at that brightness for some duration, then fade down to zero over some duration. During PB the LED will take 1.5 seconds to fade up to a brightness of 78, hold for one second, then fade down to zero over 2.5 seconds. During PLA these values will vary every two seconds within the range given in Table C.2; PLA might decide to hold for five seconds in response to a trigger, but may not hold for any time at all on a subsequent trigger after choosing a holding time of zero seconds.

3.4 Procedure

The experiment took place on the 5th and 8th of October 2018 between the hours of 10:00 and 16:00. Before the experiment, the researcher sets Aegis to PB or PLA mode, ensuring that each group of subjects is even. Multiple subjects may interact with Aegis, but only one set of physiological sensing devices are available. The subject begins the experiment at the information table near the exhibit. The brainwave and skin-conductance devices are equipped if they are not in use. The researcher leads the subject to Aegis. If the equipment is worn, one minute of data is collected while the subject is standing still with Aegis. The subject is then instructed to interact with Aegis for up to 20 minutes and return to the researcher when they are done[14]. For a second time, one minute of physiological data is collected while the subject stands still with Aegis. The researcher and subject return to the table, equipment is removed, and the subject is given the subjective experience questionnaire (see Appendix C.2.2 for the questions). The experiment is complete when the subject finishes the questionnaire.

[13] PLA utilizes a form of reinforcement learning called Deep Deterministic Policy Gradient implemented in TensorFlow (Abadi et al., 2015).

[14] All subjects returned within 20 minutes and the researcher did not have to gather any subjects from Aegis.

3.5 Analysis: SCL

3.5.1 Data Preparation and Parameters

Data was retrieved from the Empatica device using the E4 Connect Android application. The data is compiled as a set of single-channel one-minute recordings. Each subject, who is either in the PB or PLA group, contributes two recordings: *pre* and *post*. Recordings which never rise above 0.5 μS, an abnormally low conductance indicating very poor electrode connectitivity, are automatically removed from the analysis. Signal artifacts are manually removed from the recording using $EDA\ Inspector$. Recorded intervals with a relatively large negative slope, a phenomenon not explained by physiological processes governing electrodermal activity (Boucsein, 2012), are considered to be artifacts. We consider a large negative slope to be less than $-0.5\ \mu S/s$. The artifact begins when the negative slope begins, and ends when the signal visibly returns to pre-artifact levels.

Following artifact rejection, the recordings are summarized with two parameters: mean and slope (of the regression line). Notating the remaining samples as a set of tuples $\{(y_i, t_i) | 1 \leq i \leq N\}$, where the sample at time t_i has a value of y_i μS, the parameters can be calculated:

- $\text{mean} = \frac{1}{N} \sum_{i=1}^{N} y_i$
- $\text{slope} = \frac{\sum_{i=1}^{N} (y_i - \bar{y})(t_i - \bar{t})}{\sum_{i=1}^{N} (y_i - \bar{y})^2}$

These two parameters tell us different things about the signal. With the mean we can investigate a general increase or decrease of arousal within times and between groups. The slope of the regression line parameterizes the dynamics within each interval, indicating whether skin conductance was rising or falling during the interval.

3.5.2 Results: Mean

Random Effects and Model Selection

The ICC indicates that 92.50% of model variance is explained by subject grouping. A likelihood ratio test showed that a model including an interaction between time and group has the lowest AIC and is a significantly better fit compared to a model containing time and group but no interaction ($\chi^2 = 4.4422, p = .04$). Model comparisons are shown in Table 3.1. Therefore the analysis will consider the LMM which subscribes to the formula

$$\texttt{mean} \sim \texttt{time * group + 1|subject}$$

Table 3.1: Mean SCL: Model Comparison Characteristics

Model	Formula	AIC	logLik	deviance
null	$Y \sim 1 + (1\|S)$	96.752	-45.376	90.752
time only	$Y \sim T + (1\|S)$	98.376	-45.188	90.376
group only	$Y \sim G + (1\|S)$	98.540	-45.270	90.540
time and group	$Y \sim T + G + (1\|S)$	100.150	-45.075	90.150
time, group, and interaction	$Y \sim T * G + (1\|S)$	97.708	-42.854	85.708

Summary of Effects

See Figure 3.2 for an interaction plot of mean SCL for each subject. Wald tests of the fixed model coefficients (Table 3.2) to compare mean SCL in each group at each time, and their interaction, to the average mean SCL (grand mean) indicated a significant interaction between group and time:

- Subjects in (pre:PB) conditions have a significantly **higher** mean SCL
- Subjects in (pre:PLA) condition have a significantly **lower** mean SCL
- Subjects in (post:PB) conditions have a significantly **lower** mean SCL
- Subjects in (post:PLA) conditions have a significantly **higher** mean SCL

Table 3.2: Mean SCL: Fixed Effects

Effect	Estimate	SE	df	t	p	Sig
(Intercept)	6.2156	2.7216	8.0210	2.284	.05	
pre	-0.4658	0.4281	7.0530	-1.088	.31	
post	0.4075	0.3746	7.0530	1.088	.31	
PB	1.2816	2.5350	8.0267	0.506	.63	
PLA	-1.4647	2.8971	8.0267	-0.506	.63	
pre:PB	1.0132	0.4025	7.0573	2.517	.04	*
pre:PLA	-1.1579	0.4600	7.0573	-2.517	.04	*
post:PB	-0.8865	0.3522	7.0573	-2.517	.04	*
post:PLA	1.0132	0.4025	7.0573	2.517	.04	*

$* = p < .05$, $** = p < .01$, $*** = p < .001$

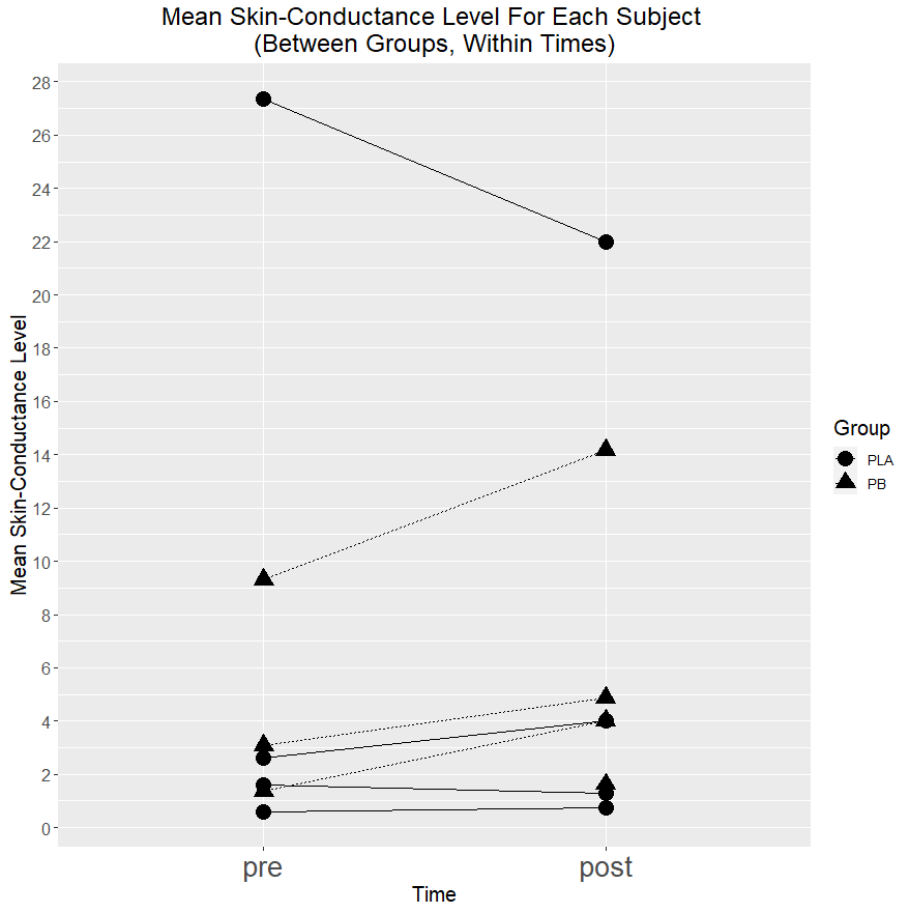

Figure 3.2: Interaction effect between behaviour group (between subjects; PB with fixed parameters and PLA with parameters varying within the ranges in Table C.2 according to the machine learning agent) and recording time (within subjects; before and after exposure) on mean SCL. Each line on the plot corresponds to a single subject and connects their *pre* and *post* values (note that one subject only has usable data in the *post* time).

3.5.3 Results: Slope

No significant results.

3.6 Analysis: EEG

3.6.1 Data Preparation and Parameters

Data from the Muse device was retrieved by listening to the `muse/eeg` OSC[15] path provided by InteraXon's `LibMuse` Android Java library[16]. The data is compiled as a set of four-channel one-minute recordings of EEG sampled at 220 Hz. Each subject, who are either in the *PB* or *PLA* group, contributes two recordings: *pre* and *post*. Signals are put through a Butterworth bandpass filter of order 3 to filter out frequencies outside of the range of interest (1 Hz to 30

[15]Open Sound Control.

[16]They appear to have dropped support for this library but documentation still lives here: https://sites.google.com/a/interaxon.ca/muse-developer-site/museio/osc-paths/osc-paths—v3-6-0.

Hz). Signal artifacts are manually removed from the recording using the EEG mode of *EDA Inspector*[17]. Recorded intervals that match easily recognizable artifact forms classified in Louis and Frey (2016), such as movements of the eyes, head, mouth, and tongue, pulse, sweat, and electrode disconnection, as well as intervals of the signal which extend more than 100 μV in absolute amplitude, are marked for removal. In some cases, signal noise from a bad electrode connection overtakes the EEG signal and results in the removal of an entire channel.

Following artifact rejection, each channel of the recording is summarized by the absolute power spectral density (PSD)[18] of canonical EEG frequency bands: delta [1 Hz to 4 Hz), theta [4 Hz to 8 Hz), alpha [8 Hz to 14 Hz), and beta [14 Hz to 30 Hz)[19]. The Lomb-Scargle method is used[20] to calculate periodograms of unevenly sampled signals[21] (Lomb, 1976; Scargle, 1982; VanderPlas, 2017; Townsend, 2010). We used the `lombscargle` function from the `AstroPy` library (The Astropy Collaboration, 2018). Combining Lomb-Scargle periodograms and Welch's method[22] we calculate a periodogram for each recording:

- partition signal into 118 one-second intervals which overlap by one half-second
- apply a Hamming window function element-wise to each interval
- calculate a Lomb-Scargle periodogram for each interval
- calculate the element-wise mean across intervals to arrive at a mean periodogram for the signal

To find the absolute power of each named frequency band, we numerically integrate by frequency for the periodogram samples that constitute that band.

Finally, we calculate the mean across channels for each band power, reducing each recording to four parameters: delta power, theta power, alpha power, and beta power.

3.6.2 Summary of Results

None of the following models produced significant model coefficients:

```
delta power ~ time * group + 1|subject

theta power ~ time * group + 1|subject

alpha power ~ time * group + 1|subject

 beta power ~ time * group + 1|subject
```

[17] This creates gaps in the data record, but the effective Nyquist frequency remains 110 Hz (see Appendix B).

[18] We use absolute PSD, rather than relative (to the subject) PSD, for the same reason that EDA recordings are not standardized by subject. Mixed models properly handle subject differences.

[19] For our discrete set of frequency points, label it S, $[i, j) = \{x \in S | i \leq x < j\}$. This is standard notation to indicate that the number on the square bracket is included in the interval, and the interval ends just before the number on the round bracket.

[20] Thanks to a day in 2015 with Hubert J. Banville at InteraXon for the idea.

[21] A simple example that explains why this is popular with the astronomical community: you want to find the orbital frequency of the moon by finding the frequency with the largest amount of power, but some nights the clouds prevent you from tracking it. As a consequence you cannot use traditional Fourier methods which require an observation of the moon at the same time every night.

[22] This combination has been called a "Lomb-Welch" periodogram (Thong et al., 2004).

3.7 Analysis: Subjective Experience Questionnaire

Subjects filled out a questionnaire after interacting with Aegis. Each question is formatted as a 7-point semantic differential scale. Some questions have been removed from the analysis (see Appendix C.2.2). The remaining questions are partitioned into Sensing, Thinking, Emotion, Autonomy, Biology, and Predictability categories. The mean of the answers for each question in a category is used as a score for that category. Independent samples t-tests[23] are performed to determine differences between the means of the PB and PLA conditions.

Six independent samples t-tests, one for each category score, test differences in mean between PB and PLA conditions. A Bonferroni correction for six tests means that any individual test shows a significant difference in means only if its p-value is less than or equal to 0.0083[24].

No significant differences in means between PB and PLA conditions were found for any category score.

3.8 Discussion

3.8.1 Results

This experiment sufferered from a small sample size due to the time limitations given by the museum. This hurts the statistical power of our analysis and makes it less likely to detect any true differences between PB and PLA. As for the effect found for mean SCL, the figures show the effect was mostly driven by the one subject in the PB condition who arrived to the experiment particularly sweaty in the first place; they had probably been wearing their coat inside the museum for a while and took it off during the experiment. Otherwise, it could be that subjects moved differently while viewing a particular condition in between SCL recordings, and that this resulted in the SCL interaction effect. The actions that triggered system activity were identical in each case (triggering any one of the proximity sensors), but the system's response differed. The response always radiated away from the triggered sensor in a similar pattern for each condition, but perhaps the varying response parameters of PLA were more likely to cause a subject to walk to multiple sensors to see if the same thing happens compared to the fixed response parameters of PB. In future studies of this type, it would be useful to track the movements of subjects while viewing the system. Despite statistical significance, we consider the results of the physiological signal analysis inconclusive.

The complete picture also includes our work described in Meng et al. (2020). There it is shown that PLA is qualitatively different from PB by outscoring PB on our measurements of engagement and interaction. Questionnaire answers show that PLA had a significantly higher Likeability score compared to PB, but there was no difference for the Anthropomorphism, Perceived Intelligence, Perceived Safety and, in particular, Animacy scores.

3.8.2 Efficacy of Mobile Biometrics

In this experiment we utilized mobile biometric sensors that are available at commercial electronics stores. Forebodingly, these sensors are generally marketed as exercise or meditation aids rather than scientific recording devices but are nevertheless increasingly popular among scientists across disciplines due to their simple and their advertised, yet somewhat deceptive, straight-out-of-the-box method of operation. The small amount of research aimed at validating the E4 finds that its EDA output does not correlate with laboratory equipment (Milstein and

[23] Also called Welch's unequal variances t-test. Not the same Welch from Welch's periodogram.

[24] because $\frac{0.05}{6} = 0.0083$

Gordon, 2020). The Muse has been shown to record various event-related potentials (ERP) (Krigolson et al., 2017) but is also less reliable than similar consumer grade products used in neuroscience research (Ratti et al., 2017).

With a proliferation of new technologies there are now many choices of recording devices spanning a wide variety of electrode styles and placements, connection methods, and data processing tools (Cruz-Garza et al. (2017) compares various EEG devices in a museum setting). At the very least, an analysis must account for these differences and be fine-tuned based on device. It is important that we develop and adhere to strict protocols for biometric data collection and analysis. In preparation for the challenges we met in the analysis, Francey et al. (2019) collected biometric data with the same devices and software used in this thesis[25]. Mobile devices suffer the magnified analogues of the same problems you see in laboratory settings. They should generally be avoided in EDA and EEG studies but they allow us to collect signals in places where the laboratory equipment cannot follow. Signal artifacts are ubiquitous; detection and removal is necessary. We prepared for data collection to fail in this way and a robust analysis method recovers whatever information is left. Studies using mobile biometric devices should aim to use many subjects to counteract the data loss[26].

[25]Results: Skin-conductance measurements with the Empatica are significantly affected by moving the wrist but we detected no difference between standing still and walking.

[26]Think of it this way: Being in a laboratory is like having a metal detector on the beach. We aren't in the laboratory, we've only got a shovel, but if we dig up enough sand we'll still find some coins.

Chapter 4

General Discussion

In this thesis we approach the study of agency and animacy by coming from the other direction. Rather than define an agent, we instead define an inanimate object and build differences from there. We explicitly parameterized what can be considered an inanimate object in the limited context of the study space, and from there we attempt to create an agent by adding or modifying parameters. In the first experiment we contend with the context of gravity and inertia, where an inanimate object must follow a zero jerk motion path, and view animate agents under the assumption that they may break these physical rules. Other studies take a similar, although not usually as explicit as is done here, assumption of context- or law-violating animate agent behaviours. It is indeed found that objects whose jerky movements breaks these rules to a high degree are rated as animate objects more often than objects which don't. In the second experiment our context becomes an interactive system whose animate-ness is dubious but whose agency is unclear. In one condition (PB) the system is imitating an agent, but its decisions are fully controlled by a human. In the other condition (PLA) the system is autonomous, making decisions that even fooled[1] the designers during testing. With full knowledge of both operating conditions, PB was predictable but PLA was not. For this reason, we internally considered PB as inanimate and PLA as animate but did not necessarily make this assumption when designing the experiment, hoping for the data to tell us so. Keeping in mind the complications of a small sample[2], we did not find any difference in our main investigation of agency using the questionnaire. In the future, we hope that studies investigating agency might follow this rigorous and explicit approach to definitions of animacy and agency.

[1] The system decided its lights should be off during an early testing session, and we thought we had broken something until we checked the activity logs.

[2] A small sample makes us less likely to find a true effect, and more likely for any outlier subject to influence the statistical models.

Bibliography

Abadi, M., Agarwal, A., Barham, P., Brevdo, E., Chen, Z., Citro, C., Corrado, G. S., Davis, A., Dean, J., Devin, M., Ghemawat, S., Goodfellow, I., Harp, A., Irving, G., Isard, M., Jia, Y., Jozefowicz, R., Kaiser, L., Kudlur, M., Levenberg, J., Mané, D., Monga, R., Moore, S., Murray, D., Olah, C., Schuster, M., Shlens, J., Steiner, B., Sutskever, I., Talwar, K., Tucker, P., Vanhoucke, V., Vasudevan, V., Viégas, F., Vinyals, O., Warden, P., Wattenberg, M., Wicke, M., Yu, Y., and Zheng, X. (2015). TensorFlow: Large-scale machine learning on heterogeneous systems. Software available from tensorflow.org.

Barr, D. J., Levy, R., Scheepers, C., and Tily, H. J. (2013). Random effects structure for confirmatory hypothesis testing: Keep it maximal. *J Mem Lang*, 68(3).

Bates, D., Mächler, M., Bolker, B., and Walker, S. (2015). Fitting linear mixed-effects models using lme4. *Journal of Statistical Software*, 67(1):1–48.

Beran, T. N., Ramirez-Serrano, A., Kuzyk, R., Fior, M., and Nugent, S. (2011). Understanding how children understand robots: Perceived animism in child–robot interaction. *Int. J. Human-Computer Studies*, 69:539–550.

Bonini, L. (2017). The extended mirror neuron network: Anatomy, origin, and functions. *The Neuroscientist*, 23(1):56–67.

Boucsein, W. (2012). *Electrodermal activity*. Springer Science + Business Media, 2 edition.

Bradley, M. M. and Lang, P. J. (1994). Measuring emotion: The self-assessment manikin and the semantic differential. *J Behav Ther Exp Psychiatry*, 25(1):49–59.

Brass, M., Schmitt, R. M., Spengler, S., and Gergely, G. (2007). Investigation action understanding: Inferential processes versus action simulation. *Current Biology*, 17:2117–2121.

Chan, M. T. K., Gorbet, R., Beesley, P., and Kulić, D. (2015). Curiosity-based learning algorithm for distributed interactive sculptural systems. *2015 IEEE/RSJ International Conference on Intelligent Robots and Systems (IROS)*, pages 3435–3441.

Chang, D. H. F. and Troje, N. F. (2009). Acceleration carries the local inversion effect in biological motion perception. *Journal of Vision*, 9(1):19:1–17.

Cruz-Garza, J. G., Brantley, J. A., Nakagome, S., Kontson, K., Megjhani, M., Robleto, D., and Contreras-Vidal, J. L. (2017). Deployment of mobile eeg technology in an art museum setting: Evaluation of signal quality and usability. *Frontiers in Human Neuroscience*, 11(527):1–18.

Dennett, D. C. (1971). Intentional systems. *The Journal of Philosophy*, 68(4):87–106.

di Pellegrino, G., Fadiga, L., Fogassi, L., Gallese, V., and Rizzolatti, G. (1992). Understanding motor events: a neurophysiological study. *Exp Brain Res*, 91:176–180.

Eyer, L. and Bartholdi, P. (1999). Variable stars: Which nyquist frequency? *Astron. Astrophys. Suppl. Ser.*, 135:1–3.

Finch, W. H., Bolin, J. E., and Kelley, K. (2014). *Multilevel Modeling Using R*. CRC Press.

Francey, A. L. Z. (2020a). *EDA Inspector*. https://github.com/afrancey/EDA-Inspector.

Francey, A. L. Z. (2020b). *EEGProcessor.py*. https://github.com/afrancey/EEG-Signal-Analysis.

Francey, A. L. Z., Grant, E., Negami, H., Srikantharajah, J., Mazumder, R., and Ellard, C. (2019). Challenges of biometric data collection. *UX+Design Conference 2019*.

Fukuda, H. and Ueda, K. (2010). Interaction with a moving object affects one's perception of its animacy. *Int J Soc Robot*, 2:187–193.

Gallese, V., Fadiga, L., Fogassi, L., and Rizzolatti, G. (1996). Action recognition in the premotor cortex. *Brain*, 119:593–609.

Gallese, V., Keysers, C., and Rizzolatti, G. (2004). A unifying view of the basis of social cognition. *TRENDS in Cognitive Sciences*, 8(9):396–403.

Gao, T., McCarthy, G., and Scholl, B. J. (2010). The wolfpack effect: Perception of animacy irresistibly influences interactive behavior. *Psychological Science*, 21(12):1845–1853.

Gao, T., Newman, G. E., and Scholl, B. J. (2009). The psychophysics of chasing: A case study in the perception of animacy. *Cognitive Psychology*, 59:154–179.

Gazzola, V., Rizzolatti, G., Wicker, B., and Keysersa, C. (2007). The anthropomorphic brain: The mirror neuron system responds to human and robotic actions. *NeuroImage*, 35:1674–1684.

Gelman, R., Durgin, F., and Kaufman, L. (1995). Distinguishing between animates and inanimates: not by motion alone. In Sperber, D., Premack, D., and Premack, A. J., editors, *Symposia of the Fyssen Foundation. Causal cognition: A multidisciplinary debate*, pages 150–182. Clarendon Press/Oxford University Press.

Giorgio, E. D., Lunghi, M., Simion, F., and Vallortigara, G. (2017). Visual cues of motion that trigger animacy perception at birth: the case of self-propulsion. *Developmental Science*, 20.

Gorbet, R., Memarian, M., Chan, M., Kulić, D., and Beesley, P. (2015). Evolving systems within immersive architectural environments: New research by the living architecture systems group. *Next Generation Building*, 2.1:31–56.

Heider, F. and Simmel, M. (1944). An experimental study of apparent behaviour. *The American Journal of Psychology*, 57:243–259.

Iacoboni, M., Molnar-Szakacs, I., Gallese, V., Buccino, G., Mazziotta, J. C., and Rizzolatti, G. (2005). Grasping the intentions of others with one's own mirror neuron system. *PLoS Biol*, 3(3):e79.

Johansson, G. (1973). Visual perception of biological motion and a model for its analysis. *Perception & Psychophysics*, 14(2):201–211.

Kaiser, M. and Proffitt, D. R. (1987). Observers' sensitivity to dynamic anomalies in collisions. *Perception & Psychophysics*, 42(3):275–280.

Kim, I. K. and Spelke, E. S. (2008). Intant's sensitivity to effects of gravity on visible object motion. *Journal of Experimental Psychology: Human Perception and Performance*, 18(2):385–393.

Krigolson, O. E., Williams, C. C., Norton, A., Hassall, C. D., and Colino, F. L. (2017). Choosing muse: Validation of a low-cost, portable eeg system for erp research. *Frontiers in Neuroscience*, 11(109):1–10.

Kuznetsova, A., Brockhoff, P. B., and Christensen, R. H. B. (2017). lmerTest package: Tests in linear mixed effects models. *Journal of Statistical Software*, 82(13):1–26.

Lüdecke, D. (2020). *sjPlot: Data Visualization for Statistics in Social Science*. R package version 2.8.3.

Leslie, A. M. (1995). A theory of agency. In Sperber, D., Premack, D., and Premack, A. J., editors, *Symposia of the Fyssen Foundation. Causal cognition: A multidisciplinary debate*, pages 121–149. Clarendon Press/Oxford University Press.

Lomb, N. R. (1976). Least-squares frequency analysis of unequally spaced data. *Astrophysics and Space Science*, 39:447–462.

Louis, E. K. S. and Frey, L. C. (2016). *Electroencephalography*. American Epilepsy Society.

Mann, S. and Janzen, R. (2014). Actergy as a reflex performance metric: Integral-kinematics applications. *2014 IEEE Games Media Entertainment*, pages 1–2.

Mann, S., Janzen, R., and Post, M. (2006). Hydraulophone design considerations: Absement, displacement, and velocity-sensitive music keyboard in which each key is a water jet. *Proc. ACM International Conference on Multimedia, October 23-27, Santa Barbara, USA*, pages 519–528.

Meng, L., Lin, D., Francey, A. L. Z., Gorbet, R., Beesley, P., and Kulić, D. (2020). Learning to engage with interactive systems: A field study on deep reinforcement learning in a public museum. *ACM Trans. on Human-Robot Interaction*.

Milstein, N. and Gordon, I. (2020). Validating measures of electrodermal activity and heart rate variability derived from the empatica e4 utilized in research settings that involve interactive dyadic states. *Frontiers in Behavioural Neuroscience*, 14(148):1–13.

Nielsen, R. H., Vuust, P., and Wallentin, M. (2015). Perception of animacy from the motion of a single sound object. *Perception*, 44:183–197.

Opfer, J. E. (2002). Identifying living and sentient kinds from dynamic information: the case of goal-directed versus aimless autonomous movement in conceptual change. *Cognition*, 86:97–122.

Ratti, E., Waninger, S., Berka, C., Ruffini, G., and Verma, A. (2017). Comparison of medical and consumer wireless eeg systems for use in clinical trials. *Frontiers in Human Neuroscience*, 11(398):1–7.

Reitsma, P. S. A., Andrews, J., and Pollard, N. S. (2008). Effect of character animacy and preparatory motion on perceptual magnitude of errors in ballistic motion. *EUROGRAPHICS*, 27(2):201–210.

Reitsma, P. S. A. and Pollard, N. S. (2003). Perceptual metrics for character animation: Sensitivity to errors in ballistic motion. *ACM Transactions on Graphics*, 24(3):537–542.

Rizzolatti, G., Fadiga, L., Gallese, V., and Fogassi, L. (1996). Premotor cortex and the recognition of motor actions. *Cognitive Brain Research*, 3:131–141.

Santos, N. S., David, N., Bente, G., and Vogeley, K. (2008). Parametric induction of animacy experience. *Consciousness and Cognition*, 17:425–437.

Saxe, R. (2005). Against simulation: the argument from error. *TRENDS in Cognitive Sciences*, 9(4):174–179.

Scaleia, B. L., Zago, M., Moscatelli, A., Lacquaniti, F., and Viviani, P. (2014). Implied dynamics biases the visual perception of velocity. *PLoS ONE*, 9(3):e93020.

Scargle, J. D. (1982). Studies in astronomical time series analysis. ii. statistical aspects of spectral analysis of unevenly spaced data. *Astrophysical Journal*, 263:835–853.

Scholl, B. J. and Tremoulet, P. D. (2000). Perceptual causality and animacy. *Trends in Cognitive Sciences*, 4(8):299–309.

Sommet, N. and Morselli, D. (2017). Keep calm and learn multilevel logistic modeling: A simplified three-step procedure using stata, r, mplus, and spss. *International Review of Social Psychology*, 191(2):203–218.

Szego, P. A. and Rutherford, M. D. (2007). Actual and illusory differences in constant speed influence the perception of animacy similarly. *Journal of Vision*, 7(12):1–7.

Szego, P. A. and Rutherford, M. D. (2008). Dissociating the perception of speed and the perception of animacy: a functional approach. *Evolution and Human Behaviour*, 29:335–342.

Te Grotenhuis, M., Pelzer, B., Eisinga, R., Nieuwenhuis, R., SChmidt-Catran, A., and Konig, R. (2016). A novel method for modelling interaction between categorical variables. *International Journal of Public Health*, pages 1–5.

The Astropy Collaboration (2018). The Astropy Project: Building an Open-science Project and Status of the v2.0 Core Package. *The Astronomical Journal*, 156:123.

Thong, T., McNames, J., and Aboy, M. (2004). Lomb-wech periodogram for non-uniform sampling [sic]. In *Proceedings of the 26th Annual International Conference of the IEEE EMBS*, pages 271–274. IEEE EMBS.

Townsend, R. H. D. (2010). Fast calculation of the lomb-scargle periodogram using graphics processing units. *The Astrophysical Journal Supplement Series*, 30(1).

Tremoulet, P. D. and Feldman, J. (2000). Perception of animacy from the motion of a single object. *Perception*, 29:943–951.

Tremoulet, P. D. and Feldman, J. (2006). The influence of spatial context and the role of intentionality in the interpretation of animacy from motion. *Perception & Psychophysics*, 68:1047–1058.

VanderPlas, J. (2017). Understanding the lomb-scargle periodogram. *arXiv*, 1703.09824.

Vaziri, S. and Connor, C. E. (2016). Representation of gravity-aligned scene structure in ventral pathway visual cortex. *Current Biology*, 26:766–774.

Weiss, A., Igelsböck, J., Tscheligi, M., Bauer, A., Kühnlenz, K., Wollherr, D., and Buss, M. (2010). Robots asking for directions – the willingness of passers-by to support robots. *2010 5th ACM/IEEE International Conference on Human-Robot Interaction (HRI)*.

Wheatley, T., Milleville, S. C., and Martin, A. (2007). Understanding animate agents: Distinct roles for the social network and mirror system. *Psychological Science*, 18(6):469–474.

Wickham, H. (2016). *ggplot2: Elegant Graphics for Data Analysis*. Springer-Verlag New York.

Woltman, H., Feldstain, A., MacKay, J. C., and Rocchi, M. (2012). An introduction to hierarchical linear modeling. *Tutorials in Quantitative Methods for Psychology*, 8(1):52–69.

Appendix A

Statistical Analysis Methods

The analyses presented in this thesis rely on linear mixed models[1] (LMM) and generalized linear mixed models (GLMM). These models have individual differences built into the model by allowing random effects for each subject. We do not need to, for instance, rationalize a choice of parameters to standardize each subject's physiological signals as would need to be done when using simple linear models. While simple linear models estimate parameters according to ordinary least squares regression, LMM estimate parameters according to maximum likelihood[2]. All analyses are done in R. (Bates et al., 2015; Finch et al., 2014; Woltman et al., 2012; Sommet and Morselli, 2017; Barr et al., 2013).

A.1 Required R Packages

- `lme4` (Bates et al., 2015) provides `lmer` objects (LMM) and `glmer` objects (GLMM).
- `lmerTest` (Kuznetsova et al., 2017) provides extra functionality for `lmer` objects, most importantly the `anova()` function for likelihood ratio tests and model comparisons.
- `wec` (Te Grotenhuis et al., 2016) is used for weighted effect coding of categorical variables for LMM with unbalanced data.
- `ggplot2` (Wickham, 2016) for general plots and `sjPlot` (Lüdecke, 2020) for plotting mixed models.

A.2 Step-by-step

Each analysis follows a three step process:

1. Random effects are examined by calculating the intraclass correlation (ICC) of the null model. ICC ranges from zero to one and indicates the proportion of model variance explained by the by-subject random intercept.

$$\text{null model} = Y_{is} \sim \gamma_0 + U_{0s} + e_{is}$$

[1] Also called multilevel models, random effects models, hierarchical linear models, etc.

[2] We did not use restricted maximum likelihood in this thesis, ie. `REML = false` when constructing the model objects.

$$ICC = \frac{\sigma_U^2}{\sigma_U^2 + \sigma_e^2} = \frac{\text{intercept variance}}{\text{intercept variance} + \text{residual variance}}$$

Logistic models do not have residuals. In this case the residual variance is taken to be $\frac{\pi^2}{3}$ (Sommet and Morselli, 2017).

The necessary information is found in the `summary()` output of the appropriate `lmer` object.

2. The best fitting model is found by comparing the AIC of all calculable models. A lower AIC indicates a better model fit. A likelihood ratio test (LRT), or multiple, comparing the model with the lowest AIC to the model(s) one step down in complexity is used to judge the significance of adding the coefficient(s). This is sometimes called an analysis of deviance. This method was chosen over a traditional F-test ANOVA since there exists no such test for logistic GLMM. For congruity among our analyses we use an LRT for both LMM and GLMM.

   The necessary information is found in the output of `anova()` from the `lmerTest` library.

3. Wald tests of each model coefficient compare the mean of each level of each categorical variable and their interaction to the grand mean. We compare to the grand mean by (weighted) effect coding of the categorical variables; unlike dummy coding, the intercept represents the grand mean rather than the effect of the reference level. To find the coefficient of the reference level we re-calculate the model while using a reference level with a known coefficient. The necessary information is found in the `summary()` output of the `lmer` object.

A.3 Explicit Description of Models Used in this Thesis

The models constructed for this thesis must examine the effect of no more than two categorical variables.

Throughout this thesis, we will adhere to the Wilkinson-like formula[3] used to specify models as `lmer` or `glmer` objects in R. In this thesis we consider all models which we can calculate: those which are neither boundary solutions nor nonconvergent as determined by the `lmer` object. In our case this results in random intercept, fixed slope models[4].

Here we notate a by-subject (S) random effects model with a dependent variable (DV) Y and categorical independent variables (IVs) X and W with $n_X + 1$ and $n_W + 1$ levels. X and W are represented in the model as a set of dummy variables $\{X_1, ..., X_{n_X}, W_1, ..., W_{n_W}\}$. Weighted effect coding of categorical variables results in the following interpretation of the multilevel

[3]It should be especially noted that the Wilkinson-type formula used by lme4 (and R in general) are ambiguous and should be interpreted based on context (in code, this context might be the calling function parameters). For example $Y \sim X + (1|S)$ can be an LMM, GLMM, have a continuous independent variable represented by X, have a categorical independent variable where X represents all dummy variables for each level, and many more context-specific model characteristics.

[4]ie. adding any random slopes results in either boundary solutions or nonconvergent models

model coefficients:

$$Y_{is} = \text{response for item } i \text{ of subject } s \tag{A.1}$$
$$\gamma_0 = \text{grand mean of responses (fixed intercept)} \tag{A.2}$$
$$\gamma_k = \text{deviation from grand mean of } k^{th} \text{ dummy variable (fixed coefficients)} \tag{A.3}$$
$$X_{kis} = \text{value of } k^{th} \text{ dummy variable of } X \text{ for item } i \text{ of subject } s \tag{A.4}$$
$$U_{0s} = \text{random intercept of subject } s \tag{A.5}$$
$$e_{is} = \text{error of item } i \text{ for subject } s \tag{A.6}$$

Table A.1 describes the models constructed in this thesis:

Table A.1: General Models

Model	lme4 Formula	Explicit Discretization
Null Model	$Y \sim 1 + (1\|S)$	$Y_{is} = \gamma_0 + U_{0s} + e_{is}$
One IV	$Y \sim X + (1\|S)$	$Y_{is} = \gamma_0 + \sum_{k=1}^{n_X} \gamma_k X_{kis} + U_{0s} + e_{is}$
Two IV	$Y \sim X + W + (1\|S)$	$Y_{is} = \gamma_0 + \sum_{k=1}^{n_X} \gamma_k X_{kis} + \sum_{l=1}^{n_W} \gamma_{n_X+l} W_{lis} + U_{0s} + e_{is}$
Interaction	$Y \sim X * W + (1\|S)$	$Y_{is} = \gamma_0 + \sum_{k=1}^{n_X} \gamma_k X_{kis} + \sum_{l=1}^{n_W} \gamma_{n_X+l} W_{lis} + \sum_{a=1}^{n_X}\sum_{b=1}^{n_W} \gamma_{c_{ab}} X_{ais} W_{bis} + U_{0s} + e_{is}$, $c_{ab} = n_X + n_W + (a-1)n_X + b$

A.4 Notes on Experiment 1 Analysis

In Experiment 1, the response variable is a binary answer. In this case it is appropriate to use a logistic linear mixed model (this may be accomplished by creating a `glmer` object with the `family` argument set to `binomial`).

To start the example, remind yourself that the case of a continuous dependent variable and one dichotomous independent variable has a model that looks like $Y_{is} = \gamma_0 + \gamma_1 X_{1is} + U_{0s} + e_{is}$. I will show the process of logistic regression given a dichotomous dependent variable and one dichotomous indepedent variable.

Denote the conditional probability that subject s rates trajectory i as animate as $P(Y_{is} = 1)$, or just P for readability. Performing logistic regression involves fitting a linear equation to the logit-transformed probability[5], also called the log-odds[6], so that it can be fit with a linear

[5]The logit function (l) and its inverse (l^{-1}): $l(x) = \log(\frac{x}{1-x})$, $l^{-1}(x) = \frac{e^x}{1+e^x}$

[6]The odds of an event $= \frac{\text{probability of event}}{\text{probability of event not happening}} = \frac{\text{probability of event}}{1-\text{probability of event}}$

equation:

$$\text{logit}(P) = \gamma_0 + \gamma_1 X_{1is} + U_{0s}$$

We fit the coefficients in the normal way. Finally, we may apply the inverse logit function (called the logistic function) to calculate the conditional probability given the coefficients.

$$P = l^{-1}(l(P)) \tag{A.7}$$

$$= \frac{e^{l(p)}}{1 + e^{l(p)}} \tag{A.8}$$

$$= \frac{e^{\gamma_0 + \gamma_1 X_{1is} + U_{0s}}}{1 + e^{\gamma_0 + \gamma_1 X_{1is} + U_{0s}}} \tag{A.9}$$

A.5 Notes on Experiment 2 Analysis

These equations are immensely simplified in Experiment 2, where each variable only has two levels and therefore only two dummy variables exist.

Table A.2: Experiment 2: Models

Model	lme4 Formula	Explicit Discretization
Null Model	$Y \sim 1 + (1\|S)$	$Y_{is} = \gamma_0 + U_{0s} + e_{is}$
One IV	$Y \sim X + (1\|S)$	$Y_{is} = \gamma_0 + \gamma_1 X_{1is} + U_{0s} + e_{is}$
Two IV	$Y \sim X + W + (1\|S)$	$Y_{is} = \gamma_0 + \gamma_1 X_{1is} + \gamma_2 W_{1is} + U_{0s} + e_{is}$
Interaction	$Y \sim X * W + (1\|S)$	$Y_{is} = \gamma_0 + \gamma_1 X_{1is} + \gamma_2 W_{1is} + \gamma_3 X_{1is} W_{1is} + U_{0s} + e_{is}$

Appendix B

Effective Nyquist Frequency of Evenly Sampled Time-Series with Gaps

We lose information about a signal when we sample it at discrete time points. In the case of uniform sampling at a fixed frequency, label it f_s, all of the available information is contained within the range $[0Hz, f_s/2Hz]$. $f_s/2$ is known as the Nyquist frequency. Practically, you must sample at a frequency that is at least twice the maximum frequency you wish to investigate. Experiment 2 requires information up to 30 Hz.

We can consider artifact-ridden EEG recordings as an unevenly sampled time series where artifacts are removed from the record. We are unable to apply the standard definition of Nyquist frequency to this case, but we can borrow the concept.

Eyer and Bartholdi (1999) suggest the following as a Nyquist frequency for unevenly sampled time-series:

Definition. *Let p be the largest value such that*

$$\forall t_i, t_i = t_1 + n_i p, \textit{where } n_i \in \mathbb{N} \tag{B.1}$$

The Nyquist frequency is then

$$\nu_{Ny} = \frac{1}{2p}$$

Let's use this definition to determine the effective Nyquist frequency when collecting data with a Muse headset at $f_s = 220$ Hz. We may assume that $t_1 = 0$.

Although there are gaps in the data record, non-artifact intervals are uniformly sampled at f_s Hz and so each sample is recorded at some multiple of $1/f_s$ seconds after the beginning of the recording. Written, this means that there exists integers n_i such that all timepoints t_i can be written as $t_i = n_i/f_s$. Therefore, $p = 1/f_s$ is *one particular* value that satisfies equation B.1. Further, it is the largest such number: $t_i - t_{n-1} = p$ in all of the regularly sampled intervals, any larger p would necessarily miss some point within these intervals.

The effective Nyquist frequency for our EEG data is then $\nu_{Ny} = f_s/2 = 110$ Hz. We can retrieve information about frequencies up to 110 Hz.

Appendix C

Materials

C.1 Experiment 1: Simulation Space and Stimuli Details

C.1.1 Notation

$$t = \text{time} \tag{C.1}$$

$$\vec{x}(t) = \text{the position of the object at time } t = \begin{bmatrix} x_1(t) \\ x_2(t) \\ x_3(t) \end{bmatrix} = \begin{bmatrix} \text{left/right} \\ \text{up/down} \\ \text{away/toward} \end{bmatrix} \tag{C.2}$$

$$\tag{C.3}$$

C.1.2 Positioning

If h is the subject's height in meters then the subject's viewpoint is located at

$$\text{head coordinates} = \begin{bmatrix} 0 \\ h \\ 0 \end{bmatrix} \tag{C.4}$$

and their feet will be at the coordinate origin

$$\text{feet coordinates} = \begin{bmatrix} 0 \\ 0 \\ 0 \end{bmatrix} \tag{C.5}$$

C.1.3 Initial Conditions

These vectors describe the ball's position when $t = 0$,

$$\vec{x_0} = \text{initial position (meters)} = \begin{bmatrix} 0 \\ 2.5 \\ 7 \end{bmatrix} \tag{C.6}$$

$$\vec{v_0} = \text{initial velocity (meters per second)} = \begin{bmatrix} 0 \\ 5 \\ -5 \end{bmatrix} \tag{C.7}$$

$$\vec{a_0} = \text{initial acceleration (meters per second}^2) = \begin{bmatrix} 0 \\ -9.8 \\ 0 \end{bmatrix} \tag{C.8}$$

C.1.4 Base Equations of Motion

The equation describing the position of an object with constant acceleration $\vec{a_0}$ and no jerk[1] at time t with initial conditions $\vec{x_0}$ and $\vec{v_0}$ is

$$\vec{x}(t) = \vec{x_0} + \vec{v_0}t + \frac{1}{2}\vec{a_0}t^2 \tag{C.9}$$

Substituting initial conditions, the base equation of motion used for the black ball in this experiment is,

$$\vec{x_{\text{base}}}(t) = \begin{bmatrix} x_1(t) \\ x_2(t) \\ x_3(t) \end{bmatrix} = \begin{bmatrix} 0 \\ 2.5 + 5t - 4.9t^2 \\ 7 - 5t \end{bmatrix} \tag{C.10}$$

In words, this motion is described:

A ball starts 7 m ahead and 2.5 m above the subject's feet, centered horizontally. It is given a velocity which points toward the subject at 5 m/s and upwards at 5 m/s. The only force acting on the object is gravity pulling down at an acceleration of -9.8 m/s^2. The ball creates a concave downward parabolic arc toward the subject. The ball is in the air for 1.39 seconds before hitting the ground[2].

C.1.5 Motion Paths with Zero Jerk

A constant acceleration is added to the base equation to modify the gravitational constant. Three motion paths are defined,

$$\text{normal gravity} = \vec{x_0} + \vec{v_0}t + \frac{1}{2}\vec{a_0}t^2$$

$$\text{low gravity} = \vec{x_0} + \vec{v_0}t + \frac{1}{2}(\vec{a_0} + \begin{bmatrix} 0 \\ 2 \\ 0 \end{bmatrix})t^2$$

$$\text{high gravity} = \vec{x_0} + \vec{v_0}t + \frac{1}{2}(\vec{a_0} + \begin{bmatrix} 0 \\ -2 \\ 0 \end{bmatrix})t^2$$

[1] ie. $\frac{d^2}{dt^2}\vec{x}(t) = \vec{a_0}$ and $\frac{d^3}{dt^3}\vec{x}(t) = \vec{0}$

[2] The ball appears in mid-air at $t = 0$ and the solutions to $x_2(t) = 0$ are $t = 1.39$ and $t = -0.37$. The negative solution occurs before the ball appears, corresponding to the other foot of the parabolic trajectory.

C.1.6 Motion Paths with Sinusoidal Jerk

A sinusoidal term is added to one particular dimension of the base equation,

$$x_i'(t) = x_i(t) + M\sin(10t), \text{ where } M \in \{0.5, 1, 2\} \text{ and } i \in \{1, 2, 3\}$$

The jerk in this dimension is equal to,

$$\frac{d^3}{dt^3}x_i'(t) = \frac{d^3}{dt^3}x_i(t) + \frac{d^3}{dt^3}M\sin(10t) \tag{C.11}$$

$$= -1000M\cos(10t) \tag{C.12}$$

Combinations of one affected dimension (i) at one magnitude (M) define nine motion paths with sinusoidal jerk (3 dimensions x 3 magnitudes). For example, the motion path defined by adding a high magnitude jerk ($M = 2$) to the left/right dimension ($i = 1$) is,

$$\vec{x_{jerk}}(t) = \begin{bmatrix} x_1'(t) \\ x_2(t) \\ x_3(t) \end{bmatrix} = \begin{bmatrix} 2\sin(10t) \\ 2.5 + 5t - 4.9t^2 \\ 7 - 5t \end{bmatrix}$$

C.1.7 Motion Paths with Constant Jerk

A cubic term is added to one particular dimension of the base equation,

$$x_i'(t) = x_i(t) + Mt^3, \text{ where } M \in \{-2, -1, -0.5, 0.5, 1, 2\} \text{ and } i \in \{1, 2, 3\}$$

The jerk in this dimension is equal to

$$\frac{d^3}{dt^3}x_i'(t) = \frac{d^3}{dt^3}x_i(t) + \frac{d^3}{dt^3}Mt^3 \tag{C.13}$$

$$= 6M \tag{C.14}$$

A combination of the value of i and the sign of M defines the direction of the constant jerk.

Table C.1: Directions of Constant Jerk Stimuli

Direction	i	sign of M
right	1	+
up	2	+
away	3	+
left	1	−
down	2	−
toward	3	−

Combinations of one affected direction at one magnitude ($|M|$) define eighteen motion paths with constant jerk (6 directions x 3 magnitudes). For example, the motion path defined by adding a high magnitude jerk ($|M| = 2$) to the toward direction is,

$$\vec{x_{jerk}}(t) = \begin{bmatrix} x_1(t) \\ x_2(t) \\ x_3'(t) \end{bmatrix} = \begin{bmatrix} 0 \\ 2.5 + 5t - 4.9t^2 \\ 7 - 5t - 2t^3 \end{bmatrix}$$

C.2 Experiment 2

C.2.1 Interactive Behaviour and Parameters of Aegis

Table C.2: Prescripted Behaviour Parameters

Parameters	Meaning	PB Value	PLA Range
T^m_{ru}, T^l_{ru}	ramp up time: the time it takes for the Moths or LEDs to increase up to their maximum value	1.5	$[0, 5]$
T^m_{ho}, T^l_{ho}	hold time: the time that Moths and LEDs are held at their maximum value	1	$[0, 5]$
T^m_{rd}, T^l_{rd}	ramp down time: the time it takes for Moths and LEDs to fade down to 0	2.5	$[0, 5]$
I_{max}	maximum percentage of duty cycle per PWM period	78	$[0, 100]$
T^m_{gap}	the time gap between the Moth starting to ramp up and the LED starting to ramp up	1.5	$[0, 5]$
T^{sma}_{gap}	the time gap between activation of each SMA arm on the nodes	0.3	$[0, 5]$
T^n_{gap}	the time gap between activation of each node during neighbour behaviour	1.8	$[0, 5]$
T^{min}_{bg}	minimum time to wait before activating background behaviour	45	$[15, 60]$
T^{max}_{bg}	maximum time to wait before activating background behaviour	90	$[60, 100]$
T_w	time to wait before trying to pick a moth or LED	5	$[0, 10]$
P	probability of successfully choosing an actuator during background behaviour	0.4	$[0, 1]$
T_{sma}	time between choosing SMAs to actuate	0.7	$[1, 5]$
T^{min}_{sw}	minimum time to wait before performing sweep	120	$[5, 200]$
T^{max}_{sw}	maximum time to wait before performing sweep	240	$[200, 400]$

The unit of all time parameters is seconds, except I_{max} is percentage and P is probability.

We have previously given the full description of the interactive behaviour and the table of modifiable parameters in Meng et al. (2020) (pp. 8-9) and it is quoted here:

"The active state is entered if any of the IR sensors is triggered. In this state, the node corresponding to the triggered sensor will first activate its local reflex behaviour. In the local reflex behaviour, the Moth, the LED and six SMAs attached to the same node as the triggered IR sensor will be activated. When a Moth is activated, it will ramp up the vibration to its maximum I_{max} over time T^m_{ru}, hold there for a period of time T^m_{ho}, then ramp down over (T^m_{rd}). After a waiting period (T^m_{gap}) following the sensor trigger, the LED on the same node is activated. It ramps up over time period (T^l_{ru}) to its maximum brightness (I_{max}), holds for a period of time (T^l_{ho}) and then gradually dims over (T^l_{rd}). At the same time, the SMAs are activated one after another separated by (T^{sma}_{gap}). A step voltage is applied to contract the SMA, after which a cooling-down time is started during which this SMA will not be activated again. The activation profile of the SMA wires is fixed in order to protect them from overheating, so these are not included in the parameterization shown in Table C.2. After the local reflex behaviour is triggered, the IR-detected event will be propagated from the triggered node to neighbouring

nodes after a delay (T^n_{gap}), until the edge nodes of the LAS are reached, causing a cascade of local reflex behaviours at each node. If no IR sensor triggering happens for a random time within $[T^{min}_{bg}, T^{max}_{bg}]$, the system goes into the background state. In this state, the LEDs and moths will randomly activate their local reflex behaviours with probability P every amount of time T_w. The SMAs are also activated independently with the same probability P every T_{sma}.

In either state, a sweep of LEDs in either direction along the longer axis of the installation happens at random time intervals within $[T^{min}_{sw}, T^{max}_{sw}]$. During the sweep, each LED activates local reflex behaviour and propagates in the direction of the sweep."

C.2.2 Subjective Experience Questionnaire

Subjects rated the degree with which they agree or disagree with each question by answering on a 7-point semantic differential scale.

Removed Questions

Questions 1-3 had subjects indicate pleasure and arousal on the Self-Assessment Manikin (Bradley and Lang, 1994). Instructions were not clear enough and subjects were filling out the manikin incorrectly or inconsistently. Questions 24-25 asked for a list of words and questions 26-27 asked for a sentence. The questions were too broad and the number of subjects too few to do further analysis. Question 23 ("How many other people were interacting with Aegis?") does not easily fall into any category, and was removed from the analysis.

Categories

Questions are split into the following categories:

Sensing

- 4. "Do you believe Aegis is aware of its surroundings?" (Not at all, Very much)
- 5. "Do you believe Aegis is aware of you?" (Not at all, Very Much)
- 6. "Does Aegis effectively use information from its environment?" (Not effective, Effective)

Thinking

- 7. "Do you believe that Aegis can be rational?" (Not at all, Very much)
- 8. "Do you believe that Aegis can be fair?" (Not at all, Very much)
- 9. "Do you believe that Aegis can be biased?" (Not at all, Very much)
- 11. "Do you believe that Aegis can have goals?" (Not at all, Very much)

Emotion

- 14. "Do you feel an emotional connection to Aegis?" (No connection, Strong connection)
- 15. "Do you believe Aegis could have an emotional connection to you?" (Not at all, Very much)
- 16. "Are you going to miss Aegis when you leave?" (Not at all, Very much)

- 17. “Do you believe Aegis could miss you when you leave?” (Not at all, Very much)

Autonomy

- 10. “Do you believe that Aegis’s behaviour depends on something that is not Aegis?” (Not at all, Very much)
- 18. “Do you believe Aegis has a mind of its own?” (Not at all, Very much)
- 21. “Does the motion of Aegis indicate that it can resist the force of gravity?” (Not at all, Very much)
- 22. “Do you believe Aegis is being controlled by something that is not Aegis?” (Not at all, Very much)

Biology

- 19. “If you were describing Aegis, to what degree would you describe it as alive?” (Not at all, Very much)
- 20. “How organic or biological was the motion of Aegis?” (Not at all, Very much)

Predictability

- 12. “Is Aegis Predictable?” (Unpredictable, Predictable)
- 13. “Does Aegis’s behaviour appear random?” (Not random, Completely random)